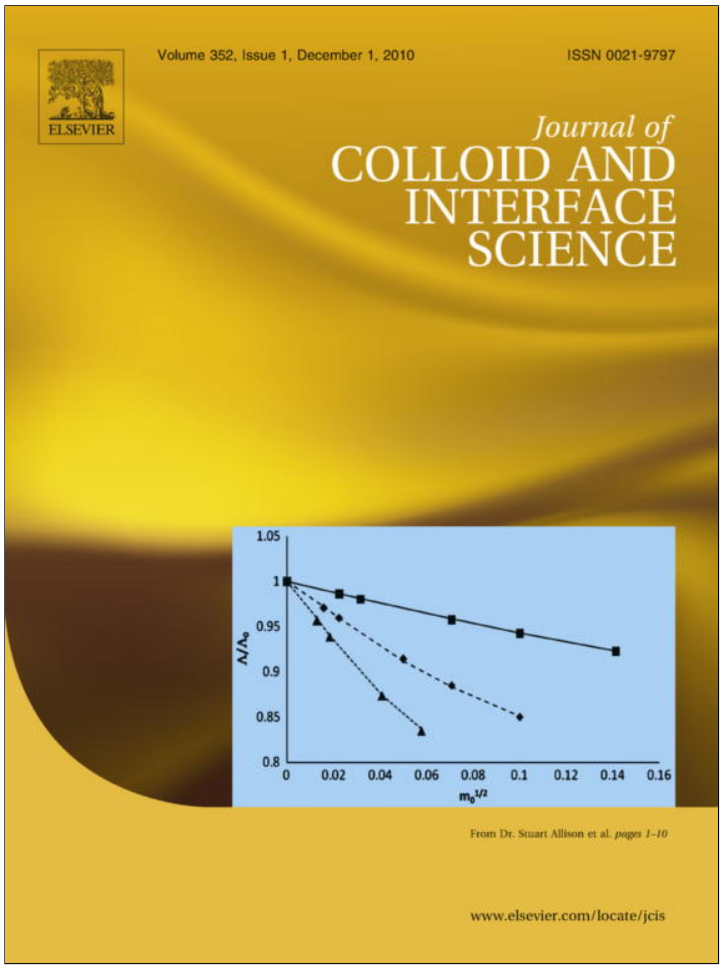

Journal of Colloid and Interface Science 352 (2010) 163–170

Contents lists available at ScienceDirect

Journal of Colloid and Interface Science

www.elsevier.com/locate/jcis

Differentiating and characterizing geminal silanols in silicas by ^{29}Si NMR spectroscopy

David K. Murray *

National Institute for Occupational Health and Safety, 1095 Willowdale Road, M/S 3030, Morgantown, WV 26505, United States

ARTICLE INFO

Article history:
Received 15 June 2010
Accepted 17 August 2010
Available online 19 August 2010

Keywords:
Silica
Silanols
NMR spectroscopy

ABSTRACT

Single and geminal hydroxyl species in silicas have been characterized using solid-state ^{29}Si NMR spectroscopy. Differentiating hydroxyl types is important in understanding their roles in chemical toxicity mechanisms for inhaled crystalline silicas responsible for silicosis. ^{1}H–^{29}Si cross polarization NMR spectroscopy has been employed to obtain ^{29}Si NMR chemical shift data and signal accrual and relaxation characteristics. Spectral deconvolution is used to examine relative single and geminal hydroxyl resonance areas for a series of representative silicas and silica gels. Silicon-containing materials examined include 1878a quartz, and 1879a cristobalite from the National Institute for Science and Technology, kaolin, and several widely used respirable silicas and silica gels. Geminal hydroxyls were observed in every case, with relative resonance areas accounting for 21–65% of total hydroxyl signals. Factors affecting relative areas measured as a function of contact time, relaxation, and surface area are discussed. Subsequent ^{29}Si and ^{31}P NMR studies of a silica coated with various sodium hydrogen phosphates show preferential single silanol–phosphate interaction for basic phosphates, and oligomerization products for acidic phosphates. Geminal hydroxyl resonance areas displayed significant error (4–17%) for low surface area silicas, limiting this method to studies exhibiting major changes in chemical or spectroscopic properties.

Published by Elsevier Inc.

1. Introduction

Occupational exposure to respirable crystalline silica remains a serious hazard for workers in the mining, construction and stone working industries [1–7]. Methods which explore silica surface chemistry are important tools in understanding the chemical mechanisms underlying the toxicity of insoluble respirable silicas [8–13]. Hydroxyl species dominate silica surfaces, terminating both crystalline and amorphous particle faces. Spectroscopic methods have been the primary means to differentiate hydroxyl species and to examine their interactions, primarily in high surface area silica gels, in order to optimize and control their catalytic and chromatographic performance. Silicon atoms in silicas are designated using a nomenclature which reports connectivity through adjacent oxygens in the tetrahedral framework. Bulk siloxane silicon (Q4) is connected to four other silicon atoms through adjacent oxygens, while silicon atoms possessing a single hydroxyl group (single silanols), occurring on particle surfaces or in internal defect sites are designated Q3, and those possessing two hydroxyl groups occurring naturally along edges and on some crystalline faces are designated Q2 (geminal silanols). Methods which differentiate Q3 and Q2 characteristics and chemistry are needed to examine specifically the relative importance of Q2 hydroxyls in silica toxicity.

NMR spectroscopy[1] has been used extensively to detect species on solid surfaces possessing NMR-active nuclei. Maciel et al. first reported solid state ^{29}Si NMR studies which detect surface silicon in a variety of silica gels [14–16]. Q3 was observed near −100 ppm (relative to tetramethylsilane) in ^{29}Si NMR spectra, while Q4 was found near −110 ppm and Q2 near −91 ppm in VCT studies. Mudrakovskii et al. [17] used ^{29}Si and ^{31}P NMR spectroscopy to study the interaction of silica gel with phosphoric acid, noting the formation of phosphates at 100 °C. Pfeiderer et al. [18] differentiated Q3 and Q2 signal areas based on varied relaxation and CP excitation parameters, attributing the multiple types observed to differing regions in silica gels. Improved Q3/Q2 differentiation was obtained by exploiting selective ^{1}H–^{1}H spin exchange and dipolar dephasing [19,20], dehydration/rehydration [15], deuterium exchange [20], and CP dynamics [21,22]. Internal silanols inaccessible to chemical reactants were differentiated from surface silanols according to hydrogen-bonding characteristics [23]. Q3:Q2

Abbreviations: NMR, nuclear magnetic resonance; ppm, parts per million; VCT, variable contact time; CP, cross polarization; SRM, standard reference material; NIST, National Institute of Standards and Technology; BET, Brunauer–Emmett–Teller (adsorption isotherm); CP/MAS, cross polarization with magic angle spinning; TTMSS, Tetrakis-trimethylsilyl silane; CT, contact time; SP, single pulse; CSA, chemical shift anisotropy.

* Fax: +1 304 285 6041.
E-mail address: DMurray@cdc.gov

0021-9797/$ - see front matter Published by Elsevier Inc.
doi:10.1016/j.jcis.2010.08.045

ratios were about 16:1 for two silica gels, indicating about 11% of the hydroxyl signal area represented Q2 silicon. ^{29}Si NMR spectroscopy was used to study spherical silica gel [24], fiberglass [25], and sol–gel microporous silica (a catalyst support) [26]. Casanovas et al. [27] presented *ab initio* calculations which confirm the chemical shift assignment of Q2 and Q3 silanols distinct from bulk Q4 siloxanes. Brown et al. [28] employed ^{29}Si VCT NMR studies to differentiate Q2 and Q3 in four amorphous and two paracrystalline opals (hydrous silicas) possessing both surface and internal silanols. In this publication, Q3 and Q2 characteristics are reported using ^{29}Si and ^{31}P NMR methods for a series of representative silica gels, natural mineral silica types and for phosphate-coated silica.

2. Materials and methods

Reference silicon-containing materials were selected for silanol detection based on their common use and toxicity. Low surface area materials examined include crystalline SRM quartz (NIST, Gaithersburg MD), SRM cristobalite (NIST), and Min-U-Sils 5™ and 40™ (US Silica Company, Berkeley Springs WV). Both SRMs exhibited a BET surface area = 4.1 m^2/g. Corresponding BET surface areas for Min-U-Sil 5 and 40 were 2.6 and <0.8 m^2/g respectively. Crystalline materials generally display both cytotoxic and fibrogenic behavior. Amorphous silica gels included Aerosil OX50™ (Degussa Corporation, Parsippany NJ) and Spherisorb™ (Waters Corporation, Taunton MA). Both amorphous materials possess high surface areas and necessarily high surface hydroxyl populations, though these materials are regarded as low or non-cytotoxic or fibrogenic. BET surface area = 52 m^2/g for Aerosil OX50 and 189 m^2/g for Spherisorb. Kaolin (Georgia Kaolin Mills, Augusta GA) is a layered clay mineral possessing surface aluminols. It has been reported as cytotoxic but not fibrogenic. BET surface area for kaolin = 13 m^2/g.

^{1}H–^{29}Si CP/MAS NMR spectroscopy was conducted according to the basic method described by Liu and Maciel for the study of fumed silica surfaces in 1996 [22]. A Bruker AVANCE DMX 300 spectrometer (7.05 T magnet) was employed for solid-state NMR spectroscopy. ^{29}Si NMR spectra were obtained at 59.6 MHz in a 7 mm CP/MAS probe. Material was studied "as received" from suppliers; supplemental drying or humidifying of silicas was not performed except as noted for coated Min-U-Sil 5. Zirconia rotors packed with 0.25–0.4 g powder were spun at 5.00 ± 0.02 kHz. ^{1}H–^{29}Si cross polarization experiments were set up using a standard sample of TTMSS, (97%, Sigma–Aldrich Company, Milwaukee WI). Following an initial ^{1}H pulse, ^{1}H and ^{29}Si B_1 fields were matched over a contact time (CT), followed by signal acquisition of the free induction decay on the ^{29}Si channel. A ^{1}H 90° pulse width of 5.1 μs was obtained using a Bruker BLAX 300 amplifier (100 W, B_{1H} = 49 kHz.) Spectral width was 6 kHz (100 ppm), centered at −100 ppm. The B_{1Si} field was adjusted to maximize the ^{29}Si signal of the quaternary TTMSS resonance intensity spin-locked under Hartmann–Hahn match conditions obtained with high power ^{1}H decoupling (150 W). This resonance served as an external chemical shift reference at −135.5 ppm. Spectra were generated by Fourier transformation of 512 data points over a 42 ms acquisition time. ^{29}Si CP spectra for silicas were obtained by signal averaging 76k scans, yielding signal to noise ratios near 10:1 for low surface area materials SRMs quartz and cristobalite as well as Min-U-Sil silicas. Signal to noise in Aerosil OX50 (52 m^2/g), Spherisorb (189 m^2/g) and kaolin was an order of magnitude better. Line widths for the resonances were typically 6–7 ppm without line broadening, and significant overlap occurred for Q2/Q3 and Q3/Q4 resonances in every case. Line broadening (100 Hz or 1.7 ppm) was employed to eliminate spurious recognition of local noise spikes during deconvolution efforts.

Initial CP studies used a 10 ms CT, though earlier studies report shorter selections of 2 ms [16], 5 ms [22] or 6–10 ms [28]. This CT selection permitted development of Q2 and Q3 signals with minor diminution due to relaxation during spin-locking. Q4 signal intensity does not reflect total siloxane silicon, since progressively longer internuclear ^{1}H–^{29}Si distances precluded the development of intensity from distant siloxane silicon in the bulk solid at any CT. Surface silicon areas were therefore not reported relative to total silicon. Q2 and Q3 intensities were diminished by saturation when recycle delays ⩽0.4 s were employed for any "as is" silica. Saturation did not occur for either Q2 or Q3 resonances in studies with recycle delays ⩾0.5 s. Separate ^{1}H progressive saturation studies yielded T_1 values < 0.2 s for hydroxyls. Recycle delays employed in the silica CP studies were therefore fixed at 1 s, with data accumulated by signal averaging 76 k scans over 23 h. This is consistent with earlier reports using 1 s recycle delays to observe surface silanols in silica gels [16,22].

Resonance areas were obtained from each ^{29}Si CP spectrum by deconvolution into three Gaussian curves using a curve fitting routine. Areas were derived by iteratively minimizing the sum of the deviations between the actual ^{29}Si spectra and the sum spectrum of all simulated resonances. Relative geminal hydroxyl silicon area (% G) reported in Table 1 is the area of the −91 ppm resonance (G) divided by the sum of G and the −100 ppm single silanol resonance area (S). The percentage of geminal hydroxyls per total hydroxyls present is estimated from these areas as well, where geminal hydroxyl area (% GOH) = 2 ∗ G/(2 ∗ G + S).

VCT studies were performed for SRM quartz and Min-U-Sil 5 materials to obtain relative silanol silicon areas (I_0) independent of contact time and the signal accrual and relaxation characteristics (T_{HSi} and $T_{1\rho}$). Six to ten contact times were selected over 0.1–22 ms range. Signal characteristics I_0, T_{HSi} and $T_{1\rho}$ were then derived by curve fitting Area vs. CT data according to:

$$\text{Area} = (I_0 * T_{1\rho})/(T_{1\rho} - T_{HSi}) * \left(e \wedge (-\text{CT}/T_{1\rho}) - e \wedge (-\text{CT}/T_{HSi})\right) \quad (1)$$

Eq. (1) is equivalent to the curve fitting equation used by Chuang and Maciel [21], and is valid when $T_{1\rho Si} \gg T_{HSi}$ and $T_{1\rho H}$. They report T_{HSi} and $T_{1\rho H}$ on the order of 1–5 ms and 40 ms, respectively, but not $T_{1\rho Si}$. $T_{1\rho Si}$ is assumed here to be much longer than $T_{1\rho H}$ because ^{1}H–^{1}H distances in silicas where adsorbed water is present are much shorter than ^{1}H–^{29}Si distances on the surface.

^{29}Si NMR SP spectra were obtained for uncoated Min-U-Sil 5 to provide an absolute quantitative comparison of single/geminal silanol and siloxane resonances relative to the TTMSS standard. These SP spectra were obtained using ^{29}Si 5.1 μs 90° pulses (B_{1Si} = 49 kHz) followed by high power ^{1}H decoupling during acquisition. Recycle delays were varied in a progressive saturation study to estimate ^{29}Si T_1 values. The recycle delay was varied over a range of 0.2 s–2 h to signal average 4–128 acquisitions. ^{29}Si T_1 values for both Q3 and Q2 resonances were less than 1 s. The Q4 resonance, however, accrued intensity over the entire delay range and the accrual curve could not be fitted to a single exponential recovery, so a single ^{29}Si T_1 could not be determined. A 4 s recycle delay was thereafter used to collect 120k data sets signal averaged over nearly a week. With this delay, less than 1% of the Q3 and Q2 resonance intensity was lost due to saturation, but the Q4 resonance intensity was greatly attenuated. The Q4 resonance area measured relative to the areas obtained for an external TTMSS standard indicated that <10% of the bulk ^{29}Si siloxane nuclei were contributing intensity to the Q4 resonance.

Coated Min-U-Sil 5 was prepared by addition of 30 micromoles of H_3PO_4, NaH_2PO_4, Na_2HPO_4, or Na_3PO_4 dissolved in 2 ml deionized H_2O to 0.4–0.5 gm aliquots of Min-U-Sil 5 in a 10 ml jar. BET surface area of Min-U-Sil 5 was 2.6 m^2/g, with a surface

Table 1
Relative geminal hydroxyl silicon areas for various silicon-containing minerals obtained by ^{1}H–^{29}Si CP/MAS NMR spectroscopy.

	Geminal hydroxyl areas		^{29}Si NMR resonance chemical shift		
	(% G)[a]	(% GOH)[b]	Q2 (ppm)	Q3 (ppm)	Q4 (ppm)
NIST SRM 1879a quartz	15 ± 10	26 ± 17	−91.4	−98.1	−106.3
NIST SRM 1878a cristobalite	15 ± 10	26 ± 17	−91.3	−101.1	−112.5
Waters Spherisorb	12 ± 3	21 ± 5	−91.2	−100.3	−109.8
Degussa Aerosil OX50	32 ± 3	48 ± 4	−90.5	−99.0	−107.9
Min-U-Sil 40	46 ± 10	63 ± 10	−91.5	−98.3	−106.8
Kaolin	0	0		−91.3/−91.8	
Min-U-Sil 5	29 ± 5	45 ± 7	−90.5	−99.4	−106.3
Min-U-Sil 5 with H_3PO_4	59 ± 5	74 ± 4	−92.3	−100.6	−106.6
Min-U-Sil 5 with NaH_2PO_4	48 ± 5	65 ± 5	−91.1	−99.0	−106.2
Min-U-Sil 5 with Na_2HPO_4	35 ± 5	52 ± 5	−92.3	−100.2	−107.0
Min-U-Sil 5 with Na_3PO_4	14 ± 5	25 ± 8	−90.2	−98.3	−105.9

[a] % G = is the ratio of the geminal silanol silicon (G) to geminal plus single silanol silicon (G + S) based on ^{29}Si NMR area deconvolution. % G = G/(G + S).
[b] % GOH is the ratio of the geminal hydroxyls to total hydroxyls derived from ^{29}Si NMR areas. % GOH = 2 ∗ G/(2 ∗ G + S).

hydroxyl concentration estimated to be 21.4 micromoles per gram based on the Kiselev–Zhuravlev constant, in which OH surface coverage = 4.9OH nm^{-2} [29]. Phosphate/hydroxyl loading was therefore about 6:1 in each case. The mixture was vortexed for 1 min, and the supernatant siphoned off after 10 min settling time. The wet solids were dried under vacuum without heating and charged to a 7 mm zirconia rotor for solid-state NMR study. ^{29}Si CP/MAS studies were conducted as per the uncoated Min-U-Sil 5 material, 76k scans accumulated with a 1 s recycle delay and a 10 ms contact time. Solid-state ^{31}P SP NMR spectra were obtained in the same 7 mm rotor and probe at 121.45 MHz. ^{31}P 90° pulse width of 5.5 μs was obtained using a Bruker BLAX300 amplifier (140 W, B_{31P} = 60 kHz). High power ^{1}H decoupling (150 W) was performed during ^{31}P signal acquisition. The spectral width was 50 kHz centered on the chemical shift of an external reference 85% D_3PO_4 sample (0.00 ppm). A 10 s recycle delay was used, and 1k data points were collected. Signal averaging of 8k scans was conducted overnight. Spin speed was varied (2.4 and 5.0 kHz) to separate isotropic resonances from spinning sidebands and visually gauge elements of ^{31}P CSA. Solid-state ^{31}P CP NMR spectra were obtained using a ^{1}H 90° pulse width of 4.4 μs followed by a 4 ms contact time matched to the first upper sideband using BLAX300 amplifiers (160 W, B_{1H} = 56 kHz). High power ^{1}H decoupling was performed during ^{31}P signal acquisition, and a 4 s recycle delay was employed.

3. Results

Relative geminal hydroxyl areas were determined for SRM quartz, SRM cristobalite, Min-U-Sils 5 and 40, and silica gels Spherisorb and Aerosil OX 50 by ^{29}Si CP NMR spectroscopy. Spectra for the crystalline silicas were acquired over roughly a 1 day period. These values are reported in Table 1. The actual and deconvoluted spectra are presented in Fig. 1. Resonances in ^{1}H–^{29}Si CP/MAS spectra were assigned to Q2–Q4 based on chemical shift. Siloxanes (Q4) are typically reported at −105 to −120 ppm, while single (Q3) and geminal (Q2) hydroxyl silicon are found at about −100 and −92 ppm respectively [16,21]. CP/MAS results reveal significant (21–65%) geminal hydroxyl silicon areas for both crystalline and amorphous silicas. Crystalline quartz and cristobalite show similar geminal hydroxyl areas but lower than Min-U-Sil 5. A repetitive study (n = 7) of Min-U-Sil 5 gave a variation of roughly 5% in the relative geminal hydroxyl silicon area. The actual signal to noise for the geminal resonance averaged 4:1 when lb = 100 Hz was applied. Without line broadening, signal to noise of 2:1 was observed, but even in this case the Q2 resonance was apparent. Amorphous silica gels Spherisorb (21%) and Aerosil OX50 (48%) possessed relative geminal hydroxyl silicon areas comparable to crystalline

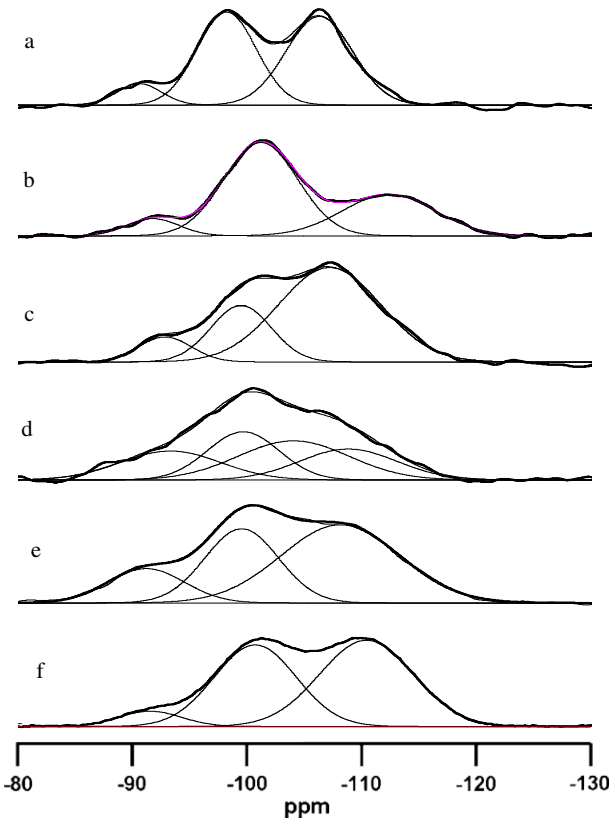

Fig. 1. ^{1}H–^{29}Si CP/MAS NMR spectra of silicas: (a) SRM quartz, (b) SRM cristobalite, (c) Min-U-Sil 5, (d) Min-U-Sil 40, (e) Aerosil OX50, and (f) Spherisorb. All spectra were obtained using a 10 ms contact time, with 1.0 s recycle delay. Sum and simulated resonance areas are superimposed on actual spectrum.

materials. Two sharp resonances were observed for kaolin (−91.3 and −91.8 ppm, not shown). These resonances are attributed to Q4 silicon atoms in SiO_4 tetrahedral sheets attached to alumina oxygen atoms in adjacent AlO_6 octahedral layers. Kaolin has no silanols, but single hydroxyls in kaolin are present as aluminols [30]. Downfield resonances observed for kaolin (−91 ppm) would appear to suggest a geminal-like Q2 environment rather than Q4. However, the change in chemical shift observed for these Q4 siloxanes (+18 ppm) was due to adjacent electron-withdrawing aluminum atoms. Geminal hydroxyl protons caused a similar downfield shift for Q2 silanol silicon, which were found about +18 ppm downfield compared to Q4 siloxanes in silicas.

A ^{29}Si NMR SP spectrum was obtained for Min-U-Sil 5 to contrast ^{29}Si Q3 and Q2 resonance areas generated by direct SP and indirect CP excitation. This spectrum is presented in Fig. 2. The relative geminal hydroxyl area in the SP spectrum is 53%, somewhat higher than that observed in the 10 ms CP spectrum. Silanol resonances were more resolved in ^{29}Si SP spectra compared to CP spectra, but decreased sensitivity made direct observation for low surface area silicas time prohibitive. ^{29}Si T_1 values were not determined for Q3 or Q2 SP resonances, but the geminal hydroxyl area was similar in a single subsequent study using a 2 s recycle delay. The Q4 area in the SP spectrum is only about 2% of the expected value based on surface area calculations, revealing a high degree of signal loss due to saturation. T_1 values for the Q4 resonances were undetermined, but appeared to be in excess of 20 min using a progressive saturation protocol to sample siloxane recovery.

A representative VCT series plot is given in Fig. 3 for Min-U-Sil 5 coated with NaH_2PO_4. Each resonance area accrues and decays at rates determined by ^{1}H–^{29}Si dipolar interactions. Q3 and Q2 resonances reached maxima (3–5 ms) at shorter CTs than Q4 resonances (6 ms or more). The Q2 resonance decayed more quickly than the Q3 resonance. The relative geminal hydroxyl area for the 10 ms contact time data set was 54%, similar to the 52% area obtained prior to the VCT series. Q2 resonance areas were greater at shorter CTs, and the rate of Q2 resonance decay appeared faster than that of the Q3 resonance. VCT studies were necessary to determine resonance areas independent of contact time for geminal silicon area determination, though the areas obtained for CT = 3 ms were within experimental error of the maximum areas observed.

VCT studies were employed to determine relative geminal hydroxyl area independent of CT for quartz, Min-U-Sil 5, and for Min-U-Sil 5 coated with NaH_2PO_4. These percentages and related CP characteristics are presented in Table 2. CT-independent values were significantly higher than the prior results at 10 ms in each case. However, 3 ms data nearly matched the CT-independent data for these three samples, and was consistent with the SP data obtained for the uncoated Min-U-Sil 5. The 10 ms data appears to underreport the relative geminal hydroxyl areas by 20–50%.

The products of Min-U-Sil 5 with simple phosphate anion coatings were examined by ^{29}Si and ^{31}P NMR spectroscopy. ^{29}Si CP/MAS NMR spectra are presented in Fig. 4, with chemical shift data listed in Table 1. Q3 and Q2 resonances persist in every case, with relative increases in geminal hydroxyl areas in most cases. Na_3PO_4

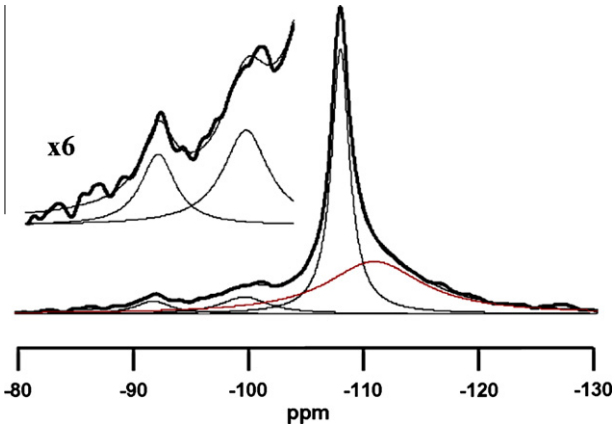

Fig. 2. ^{29}Si SP MAS NMR spectrum of Min-U-Sil 5. The spectrum was obtained using a 4 s recycle delay over 2 days. It was deconvoluted into four components: geminal (−91 ppm) and single (−100 ppm) silanols and two siloxanes (−107, −111 ppm). Geminal area is 36% of the total silanol area. Silanols are highlighted in the 6× expanded region. Actual siloxane area is attenuated by a factor of 50–100 due to saturation.

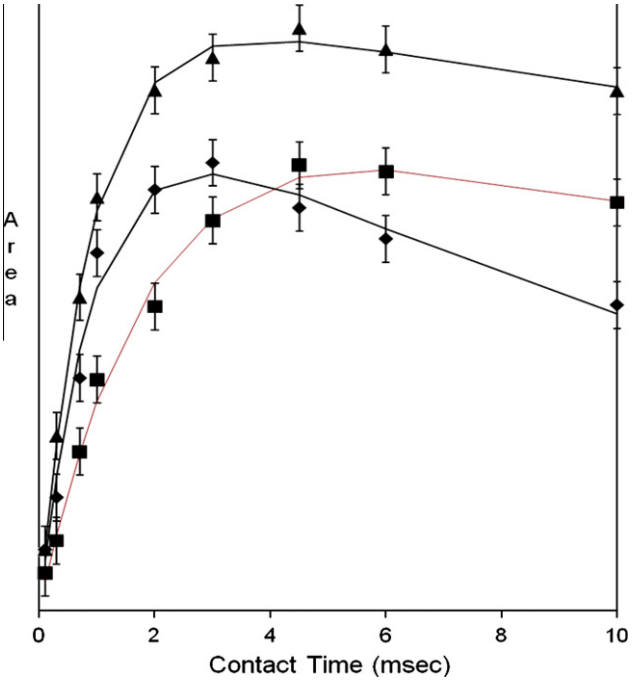

Fig. 3. Variable contact time series for Min-U-Sil 5 with a NaH_2PO_4 coating. ♦ geminals, ▲ single silanols, ■ siloxanes. Silanol resonances reach maxima (3–5 ms) at shorter contact times than those of siloxanes (6 ms or more). The geminal silanol resonance decays more quickly than single silanol resonances.

coating on Min-U-Sil 5 caused a sharpening of the Q2 resonance and a severe broadening for the Q3 resonance.

Complementary ^{31}P NMR spectra of these four phosphate coatings on Min-U-Sil 5 are presented in Figs. 5 and 6. Fig. 5 displays ^{31}P NMR spectra revealing the products of phosphate coating along with ^{31}P NMR spectra of the corresponding pure phosphate species in the region +25 to −25 ppm. These spectra revealed the formation of increasingly acidic phosphates in each case, seen as upfield chemical shifts to more acidic products. Phosphoric acid (H_3PO_4) on Min-U-Sil 5 (Fig. 5a) yielded resonances at −1.4 and −5.8 ppm, broader and upfield from the pure acid which produces a sharp resonance at 0.00 ppm, and which would produce downfield resonances when buffered in water. Upfield resonances at <0 ppm may be attributed to either surface bound phosphates on acidic sites or unbound phosphate oligomers such as $H_xP_2O_7$. This upfield resonance coincides with an additional resonance at −84 ppm in the corresponding ^{29}Si NMR spectrum (Fig. 4b). The loss of relative area for Q3 suggests it is involved.

NaH_2PO_4 on Min-U-Sil 5 (Fig. 5c) yielded a resonance at +0.4 ppm, upfield from that of the pure solid +2.0 ppm. The pure Na_2HPO_4 salt produced an isotropic resonance at +6.4 ppm, while on Min-U-Sil 5, a broad resonance with maxima at +6.7 and +3.6 ppm was observed (Fig. 5e). Na_3PO_4 on Min-U-Sil 5 yielded a broad asymmetric resonance with maxima at +6.5, and +4.6, ppm, compared to the single resonance at +7.6 ppm observed for the pure basic solid. These resonances are consistent with the formation of HPO_4^{2-}, $H_2PO_4^-$ or their sodium salts.

Fig. 6 presents ^{31}P NMR spectra of the coating products over a 200 ppm range. The spectra were obtained at both a higher (5.0 kHz) and lower (2–2.4 kHz) spin speed to differentiate isotropic resonances from spinning sidebands and to give a rough indication of CSA for the phosphates coatings over the central 200 ppm range presented. Phosphoric acid (H_3PO_4) on Min-U-Sil 5 (Fig. 6a and b) produces a CSA range of at least 100 ppm for the adsorbed phosphate, significantly different from a dispersed intact phosphoric acid species.

Table 2
Geminal hydroxyl silicon characterization for selected silicas from ^{29}Si CP VCT Studies.

	Min-U-Sil 5 Uncoated		Min-U-Sil 5 NaH_2PO_4		SRM Quartz Uncoated	
	% G	% GOH	% G	% GOH	% G	% GOH
Relative geminal hydroxyl area						
From VCT I_0 (CT independent)	35	52	48	65	29	45
From VCT 3 ms areas	36	53	45	62	30	46
From SP areas	36	53				
From VCT 10 ms areas	29	45	37	54	20	33
From prior series 10 ms areas (Table 1)	29 ± 5%	45 ± 7%	35 ± 5%	52 ± 5%	15 ± 10%	26 ± 17%
^{29}Si accrual/relaxation characteristics						
Geminal silanol T_{HSi} (ms)		1.1		1.1		2.1
Geminal silanol $T_{1\rho}$ (ms)		14.8		15.7		10.5
Single silanol T_{HSi} (ms)		1.6		0.9		2.1
Single silanol $T_{1\rho}$ (ms)		26.3		60.5		26.8

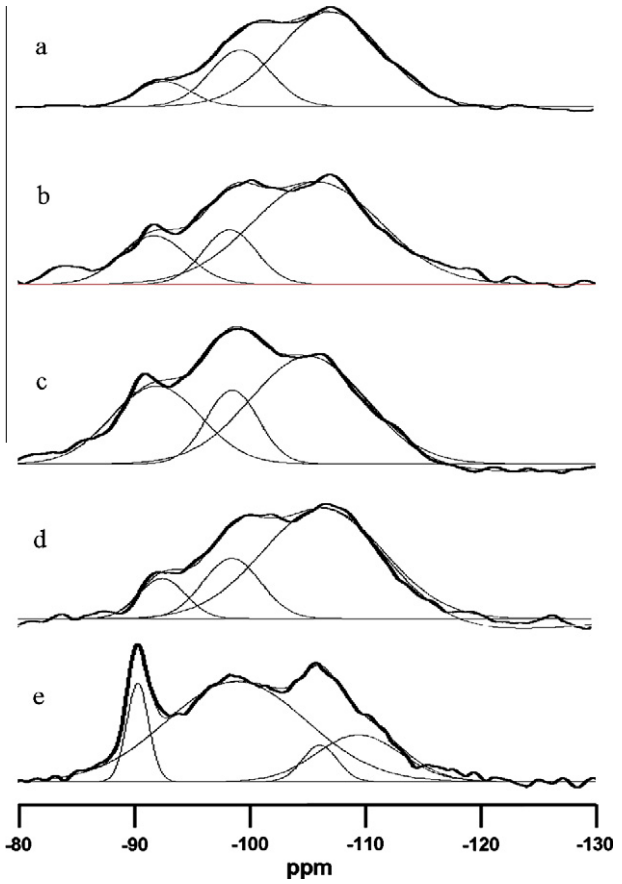

Fig. 4. ^{1}H–^{29}Si CPMAS NMR spectra of uncoated and phosphate-coated Min-U-Sil 5. Coating type: (a) uncoated, (b) H_3PO_4, (c) NaH_2PO_4, (d) Na_2HPO_4, and (e) Na_3PO_4. All spectra were obtained using a 10 ms contact time, with 1.0 s recycle delay. Sum and simulated resonance areas are superimposed on actual spectrum.

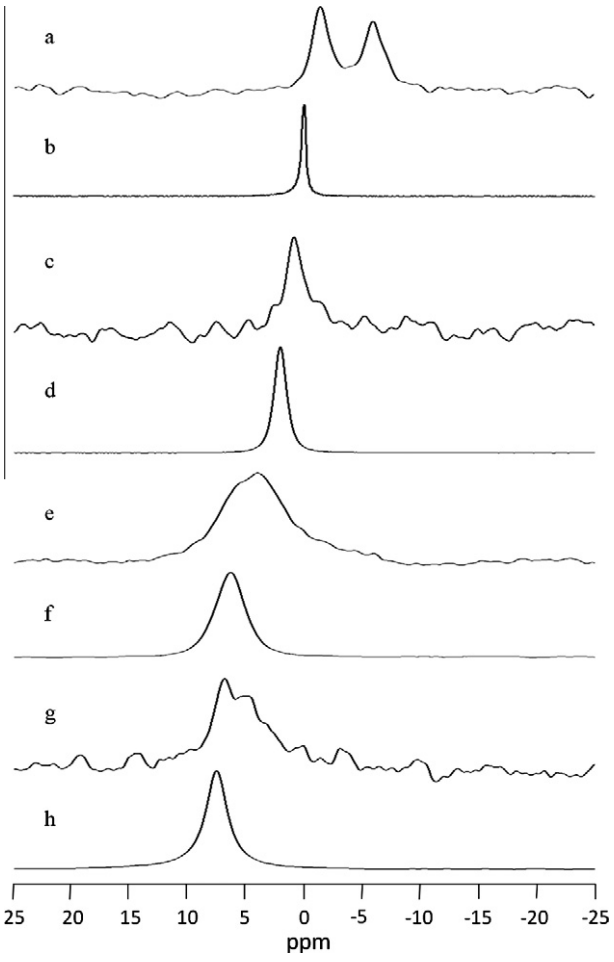

Fig. 5. ^{31}P SP NMR spectra of phosphate coatings on Min-U-Sil 5 and corresponding pure phosphates: (a,b) H_3PO_4, (c,d) NaH_2PO_4, (e,f) Na_2HPO_4, (g,h) Na_3PO_4. Rotor spin speed was 5.0 kHz (41 ppm). 8 k to 64 k scans were acquired using a 10 s recycle delay for the coated Min-U-Sil 5s, while 100 scans were acquired for the pure phosphates.

The NaH_2PO_4 coating displayed an equally broad CSA (Fig. 6c and d), while Na_2HPO_4 (Fig. 6e and f) was noticeably narrower (~80 ppm) Both pure salts exhibit CSAs on the order of 200 ppm. CSA for the Na_3PO_4 coating was less than 50 ppm, on the same order as the pure solid. The CSA pattern observed upon phosphoric acid coating differed in range from the pure acid, confirming surface distribution and product formation. CSA ranges observed for Min-U-Sil 5s coated with sodium-containing phosphates did not differ significantly from the pure solids, and were less useful in characterizing surface phosphate deposition than the upfield chemical shift changes consistently observed.

Figs. 6g and j present ^{31}P NMR spectra obtained using ^{1}H–^{31}P cross polarization rather than single pulse acquisition. In each spectrum a single resonance at about +6.6 ppm is observed, assigned to surface-adsorbed HPO_4^{2-}. Resonance intensities in the cp spectra would be skewed towards species with favorable ^{1}H–^{31}P dipolar interactions. The lack of intensity observed for $H_2PO_4^-$ species in the region +3.5 ppm to +2.0 ppm in these spectra suggests that intensities in CP spectra may result only from

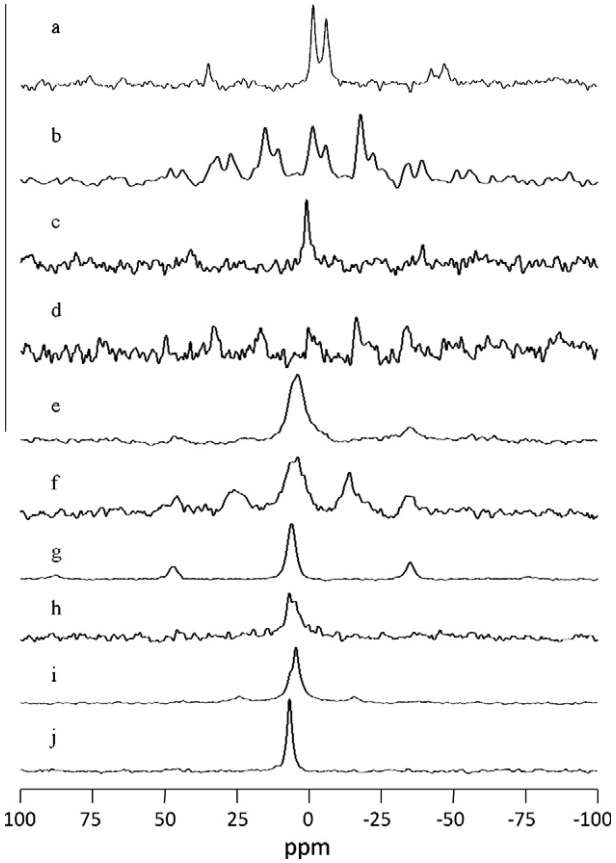

Fig. 6. ^{31}P NMR spectra of phosphate-coated Min-U-Sil 5 (a and b) H_3PO_4, (c and d) NaH_2PO_4 (e–g) Na_2HPO_4, (h–j) Na_3PO_4. Rotor spin speed was 5.0 kHz (41 ppm) in the topmost spectra (a, c, e, h) and 2.0–2.4 kHz (16–20 ppm) in the bottommost spectra (b, d, f, i). Isotropic resonances are found in the region +10 to −10 ppm, with sidebands projected up and downfield to fill the CSA envelope. 8k–64k scans were acquired using a 10 s recycle delays for these SP studies. ^{1}H–^{31}P CP NMR spectra for Na_2HPO_4 (g) and Na_3PO_4 (j)-coated Min-U-Sil 5 reveal a means of differentiating and discriminating products according to ^{1}H–^{31}P dipolar interactions in solid state spectra.

polarization transfer from surface hydroxyls rather than protons on phosphates. These results suggest a rigorous study of a stoichiometric coating including characterization of CP dynamics to differentiate roles for protonated phosphates and surface hydroxyl species.

4. Discussion

Geminal and single hydroxyl silicon were detected by ^{1}H–^{29}Si CP/MAS NMR in low surface area silicas at sufficient signal to noise to determine relative geminal and single hydroxyl areas. The variation in relative geminal hydroxyl area for the Aerosil OX50 (32%) and Spherisorb (12%) silica gels was consistent with values reported earlier for the gels Cab-O-Sil HS-5 (32%) and Fisher S-679 (14%) [16]. Geminal hydroxyl silicon areas in crystalline silicas were found in roughly the same range, though the surface area and silanol areas were 1–2 orders of magnitude lower than in amorphous materials. Relative geminal hydroxyl areas observed were not associated or predictive of known disease risk, as hydroxyls from amorphous or crystalline regions were not differentiated. However, the presence of significant percentages of geminal hydroxyls in crystalline silicas suggests that their specific activity in any proposed mechanisms of toxicity for silicas must be considered, since their area was above 20% in every case. Experimental error (5–10%) was a significant concern for this method, and low signal sensitivity and resolution limited its utility for low surface area silicas to studies where major chemical or spectroscopic changes occur. Even for the two silica gels, error was on the order of 2–3% from the line broadening and deconvolution processes.

In this study, silica materials were studied "as received" to detect silanols as they would occur upon deposition *in vivo*. Previous works have shown that removal of surface water by heating or evacuation improved surface hydroxyl resolution enough to quantify silanol types when monitored by solid-state ^{1}H NMR spectroscopy [22,23]. These efforts permitted differentiation of silanol types according to hydrogen-bonding characteristics. In the present study however, silicas were studied "as received" to avoid the inadvertent dehydroxylation of the surface hydroxyls and any associated error in relative geminal hydroxyl area. Solid-state ^{1}H NMR spectra were obtained to examine resolution in "as received" materials and to attempt resonance deconvolution to differentiate surface hydroxyls from water. The spectral features observed for water in multiple environments in these low surface area silicas were however, complex and unresolved. Spectroscopic methods which improve silanol selectivity in this native environment were not attempted and were beyond the scope of this study. A mild deuterium exchange was performed on SRM quartz to differentiate internal (inaccessible) silanols from surface species, and the percentage of resonance areas remaining was determined for the deuterated SRM quartz compared to the natural abundance material. About 20% of original Q2 and 15% of Q3 areas remained for the deuterated material, studied after three exchanges with liquid D_2O and subsequent drying at ambient temperatures. The relative geminal hydroxyl area was somewhat higher (42%) in the deuterated material, revealing the presence of significant geminal species in internal or defect sites, though the effect of signal accrual or relaxation in the areas deconvoluted from the CT = 10 ms CP spectrum was not determined. Though a portion of silanol sites are inaccessible to molecular probes, deuterium exchange studies would be needed to account for those internal sites not participating in surface hydroxyl coating or reaction studies.

A study of silica–phosphate interactions was conducted to evaluate the ^{29}Si CP method as a means of differentiating surface geminal and single hydroxyl reactions. The single loading chosen for the coating phosphates provided a qualitative product assessment in this case, demonstrating the technique for a single respirable silica. Phosphate-coated Min-U-Sil 5 was prepared by evacuation of damp powder at ambient temperature after exposure to a supernatant phosphate solution subsequently removed by suction. ^{29}Si spectral changes revealed weak and incomplete interactions between hydroxyls and phosphates, with the greatest changes occurring for more basic phosphates, interacting with weakly acidic silanols. ^{31}P NMR spectra confirmed phosphate interaction by the appearance of resonances upfield from the pure phosphate resonance in each case. The greatest ^{29}Si spectral changes occurred for the Na_3PO_4 coated Min-U-Sil 5 (Fig. 4d), where the Q2 resonance sharpened, the Q3 resonance broadened, and the Q4 siloxane resonance was greatly diminished in intensity. It is unclear if this was a consequence of the Si–O–P covalent bond formation or a change in signal accrual or relaxation characteristics for silanols in the CP study. The loss of Q4 area suggests that it is a consequence of the lack of phosphate protons rather than covalent Si–O–P formation. The relatively narrow ^{29}Si spectral region did not sample below −150 ppm, so the formation of octahedral silicon compounds was unobserved. Mudrakovskii et al. [17] reported formation of the phosphoric acid product at 100 °C. A corresponding study with Na_3PO_4 coating of kaolin shows little change in the aluminol intensity observed by ^{29}Si CP NMR, though phosphate products consistent with Al–O–P formation were present in ^{31}P spectra (a resonance at −22 ppm). These results provide a rough indication that geminal hydroxyls were less active in phosphate interactions,

and that their differing reaction may be monitored by ^{29}Si NMR spectroscopy in low surface area silicas.

Murashov, et al. report a 5% geminal hydroxyl site density from calculations of pristine α-quartz crystal surfaces based on the natural distribution of hydroxyl types on quartz crystal faces [31]. Geminal hydroxyl site density on fractured materials was threefold higher than the natural site density (14%). Crystalline SRM quartz was found in the present study to possess a higher relative geminal hydroxyl area in NMR studies, which may be a function of material grinding or other preparation procedures, or deviation from the calculated crystal face distributions. The Min-U-Sils likewise displayed higher relative geminal hydroxyl areas than those obtained by the computational method for α-quartz. NIST reports that SRM quartz and cristobalite are prepared by crushing and jet-milling to achieve specific particle size characteristics, by acid washing, and by ignition at 500 °C. The higher relative geminal area observed may be the result of such processing. These processes likely contribute to increased relative geminal hydroxyl areas by generating additional geminal hydroxyls on freshly fractured surfaces or through the loss of vicinal single hydroxyls by dehydroxylation at elevated temperatures. Both Min-U-Sils show higher relative geminal areas than those predicted from α-quartz calculations, though processing procedures for these materials are not described. Geminal hydroxyls were present in amorphous silicas though there may be structural differences not distinguished by NMR which account for reported toxicity differences between amorphous and crystalline silicas.

A difference in phosphate interaction was observed for geminal and single hydroxyl species in Min-U-Sil 5. Though preliminary, it suggests that geminals may remain available in inhaled respirable crystalline silicas upon inhalation and subsequent surfactant coating. Geminal hydroxyls did not interact with phosphates in these studies, though they are reportedly active sites in other studies. Computational studies have yielded different energetics and intermediates for geminal and isolated single hydroxyl radical reaction on differing surfaces [32] and that the silicon atoms of geminal hydroxyls were the preferred sites for radical attack [33]. High fibrogenic potential of crystalline silicas was conjectured to be the result of geminal hydroxyl silanol species, either naturally occurring or enhanced by reaction of surface radical species with water. Geminal hydroxyls as more reactive than isolated or vicinal single silanols: they underwent deprotonation, hydrolysis and silylation reactions easier than single hydroxyls, and also induced hydrolysis of phosphoesteric linkages more easily [34]. Iarlori et al. [35] report calculations for the surfaces of cristobalite to model silylation adhesion processes. The (1 0 0) and (1 1 1) faces of cristobalite were studied as models for amorphous silica surface species, as these faces are selectively populated with geminal and isolated hydroxyls respectively. They concluded that the geminal hydroxyls were the likely silylation reaction sites. Similarly, a range of surface energies was calculated by Murashov for the various pristine quartz surface faces, and the energies of the faces changed in order and intensity upon hydrolysis [36]. These calculations suggested that there are differences in hydrophilicity for quartz faces corresponding to differential vicinal/isolated areas. Murashov later concluded that geminal hydroxyls are also likely formed by surface cleavage processes [37].

Cytotoxic behavior is mitigated when crystalline silicas and kaolin are coated with phospholipids. The preference for single hydroxyl–phosphate interaction suggests that further examination of the chemical reactivity of the intact geminal hydroxyls on coated silicas is warranted. Geminal hydroxyl species were involved in surface radical generation and catalysis of phosphoesteric linkages, and may be determinates of coating integrity and the return of cytotoxic behavior observed in *in vitro* systems. Though the ^{29}Si CP NMR spectroscopic method employed here is limited by sensitivity and by deconvolution requirements, major changes in relative geminal hydroxyl areas may be detected to understand geminal hydroxyl chemistry and its role in silica toxicity and amorphous gel modification.

5. Conclusions

^{1}H–^{29}Si CP/MAS NMR provides a means of differentiating relative geminal and single hydroxyl areas in silicas. Geminal hydroxyls displayed significant relative hydroxyl areas (21–65%) in both crystalline and amorphous silicas in ^{29}Si CP studies using a resonance deconvolution technique. VCT studies yielded CT-independent areas that were significantly higher than those obtained from a single ten ms CT. Single three ms contact time spectra most closely reflected VCT results. Signal accrual and relaxation time constants for both surface silanol types are reported. Relative hydroxyl areas determined by CP are comparable to those observed using direct ^{29}Si single pulse NMR in Min-U-Sil 5. Geminal hydroxyl areas displayed significant error (4–17%) for low surface area silicas, limiting the utility of this method to studies expected to exhibit major changes in chemical or spectroscopic properties.

Coating studies suggest phosphates interacted preferentially with single hydroxyl sites in Min-U-Sil 5, with ^{31}P NMR chemical shift changes indicating phosphate anion protonation or hydroxyl association. Further studies of geminal hydroxyl reactivity are needed to verify possible roles in surface chemical processes which may be responsible for cytotoxic and fibrogenic behavior in both uncoated and coated crystalline silicas. Also needed are efforts to understand the differences in geminal distribution or chemistry giving rise to low or non-toxic behavior in amorphous silica gels.

References

[1] National Institute for Occupational Safety and Health (NIOSH), Hazard Review: Health Effects of Occupational Exposure to Respirable Crystalline Silica, DHHS (NIOSH) Publication No. 2002-129, 2002, pp. 89–91.
[2] K. Linch, Appl. Occup. Environ. Hyg. 17 (2002) 209.
[3] V.C. Antao, G.A. Pinheiro, J. Kavakama, M. Terra-Filho, Am. J. Ind. Med. 45 (2004) 194.
[4] V. Castronova, in: V. Castronova, V. Vallyathan, W.E. Wallace (Eds.), Silica and Silica-induced Lung Diseases, CRC Press, Boca Raton, 1996, pp. 79–89.
[5] L.N. Daniel, Y. Mao, T.-C.L. Wang, C.J. Markey, S.P. Markey, X. Shi, U. Saffiotti, Environ. Health 71 (1995) 60–73.
[6] K. Donaldson, P.J.A. Borm, Ann. Occup. Hyg. 42 (1998) 287–294.
[7] B. Fubini, Ann. Occup. Hyg. 42 (1998) 521–530.
[8] R.P.F. Schins, R. Duffin, D. Höhr, A.M. Knaapen, T. Shi, C. Weishaupt, V. Stone, K. Donaldson, P.J.A. Borm, Chem. Res. Toxicol. 15 (2002) 1166–1173.
[9] J. Harrison, J.-Q. Chen, W. Miller, W. Chen, E. Hnizdo, J. Lu, W. Chisholm, M. Keane, P. Gao, W. Wallace, Am. J. Ind. Med. 48 (2005) 10–15.
[10] B. Fubini, G. Zanetti, S. Altilia, R. Tiozzo, D. Lison, U. Saffiotti, Chem. Res. Toxicol. 12 (1999) 737.
[11] Z. Elias, O. Poirot, M.C. Daniere, F. Terzetti, A.M. Marande, S. Dzwigaj, H. Pezerat, I. Fenoglio, B. Fubini, Toxicol. in Vitro 14 (2000) 409.
[12] B. Fubini, I. Fenoglio, R. Ceschino, M. Ghiazza, G. Martra, M. Tomatis, P. Borm, R. Schins, J. Bruch, Int. J. Hyg. Environ. Health 207 (2004) 89.
[13] I. Fenoglio, A. Croce, F. Di Renzo, R. Tiozza, B. Fubini, Chem. Res. Toxicol. 13 (2000) 489.
[14] G.E. Maciel, D.W. Sindorf, J. Am. Chem. Soc. 102 (1980) 7606.
[15] D.W. Sindorf, G.E. Maciel, J. Am. Chem. Soc. 105 (1983) 1487.
[16] M.L. Miller, R.W. Linton, G.E. Maciel, B.L. Hawkins, J. Chromatogr. 319 (1985) 9.
[17] I.L. Mudrakovskii, V.M. Mastikhin, N.S. Kotsarenko, V.P. Shmachkova, Kinet. Catal. 29 (1988) 165.
[18] B. Pfeiderer, A.E. Bayer, L. van de Ven, J. de Haan, C. Cramers, J. Phys. Chem. 94 (1990) 4189.
[19] I-S. Chuang, D.R. Kinney, C.E. Bronnimann, R.C. Ziegler, G.E. Maciel, J. Phys. Chem. 96 (1992) 4027.
[20] I.-S. Chuang, D.R. Kinney, G.E. Maciel, J. Am. Chem. Soc. 115 (1993) 8695.
[21] I.-S. Chuang, G.E. Maciel, J. Am. Chem. Soc. 118 (1996) 401.
[22] C.C. Liu, G.E. Maciel, J. Am. Chem. Soc. 118 (1996) 5103.
[23] J.-B.d. de la Caillerie, M.R. Aimeur, Y.E. Kortobi, A.P. Legrand, J. Colloid Interface Sci. 194 (1997) 434.
[24] A.B. Scholten, J.W. de Haan, H.A. Claessens, L.J.M. van de Ven, C.A. Cramers, Langmuir 12 (1996) 4741.
[25] K.V. Romanenko, O.R. Lapina, L.G. Simonova, J. Fraissard, Phys. Chem. Chem. Phys. 5 (2003) 2686.

[26] C. Cannas, M. Casu, A. Musinu, G. Piccaluga, J. Non-Cryst. Solids 351 (2005) 3476.
[27] J. Casanovas, F. Illas, G. Pacchioni, Chem. Phys. Lett. 326 (2000) 523.
[28] L.D. Brown, A.S. Ray, P.S. Thomas, J. Non-Cryst. Solids 332 (2003) 242.
[29] L.T. Zhuravlev, Colloids Surf., A 173 (2000) 1.
[30] C.E. White, J.L. Provis, D.P. Riley, G.J. Kearley, J.S.J. van Deventer, J. Phys. Chem. B 113 (2009) 6756.
[31] V. Murashov, M. Harper, E. Demchuk, J. Occup Environ. Hyg. 3 (2006) 718.
[32] R. Konecny, S. Leonard, X. Shi, V. Robinson, V. Castronova, J. Environ. Pathol. Toxicol. Oncol. 20 (Suppl. 1) (2001) 119.
[33] R. Konecny, J. Phys. Chem. B 105 (2001) 6221.
[34] V.V. Murashov, J. Mol. Struct. 650 (2003) 141.
[35] S. Iarlori, D. Ceresoli, M. Bernasconi, D. Donadio, M. Parrinello, J. Phys. Chem. B 105 (2001) 8007.
[36] V.V. Murashov, J. Phys. Chem. B 109 (2005) 4144.
[37] V.V. Murashov, E. Demchuk, Surf. Sci. 595 (2005) 6.